International Journal of Nanoelectronics and Materials
IJNeaM
ISSN 1985-5761 | E-ISSN 2232-1535

Optimal modeling of perovskite solar cell with graphene oxide as hole transport layer using L_{32} (2^8) Taguchi design

Khairil E. Kaharudin 1[a,b], Nabilah A. Jalaludin[a], Fauziyah Salehuddin 2[a]*, Faiz Arith[a], Anis S. M. Zain 3[a], Ibrahim Ahmad 4[c], Siti A. M. Junos 5[a] and Abdul H. Afifah Maheran 6[a]

[a]*Micro & Nano Electronics (MiNE), CeTRI, Faculty of Electronics and Computer Technology and Engineering, Universiti Teknikal Malaysia Melaka, Hang Tuah Jaya, Durian Tunggal, 76100 Melaka*
[b]*Faculty of Engineering and Built Environment, Lincoln University College (Main Campus), Wisma Lincoln, 47301 Petaling Jaya, Selangor*
[c]*College of Engineering (CoE), Universiti Tenaga Nasional (UNITEN), 43009 Kajang, Selangor*

∗Corresponding author. Tel.: +606-2702361; e-mail: fauziyah@utem.edu.my

Received 12 December 2022, Revised 31 July 2023, Accepted 14 August 2023

ABSTRACT

Material parameter variations are one of the main contributors affecting the performance of solar cell devices, thus, Taguchi design is employed to optimize the material parameters in attaining maximum power conversion efficiency (PCE). This paper discusses the optimal modeling of the Perovskite solar cell (PSC) with graphene oxide (GO) hole transport layer (HTL) using L_{32} (2^8) Taguchi design. The device simulation is conducted using a solar cell capacitance simulator (SCAP), whereas the L_{32} (2^8) Taguchi design is used for device optimization. The final results reveal that the L_{32} (2^8) Taguchi design has significantly optimized the device parameters in which FTO thickness, FTO donor concentration, TiO_2 thickness, TiO_2 donor concentration, $CH_3NH_3PbI_{3-x}Cl_x$ thickness, $CH_3NH_3PbI_{3-x}Cl_x$ donor concentration, GO thickness and GO acceptor concentration are predictively set to 0.1 µm, 1 x 10^{20} cm^{-3}, 0.03 µm, 1 x 10^{20} cm^{-3}, 0.9 µm, 1 x 10^{20} cm^{-3}, 0.03 µm and 1 x 10^{20} cm^{-3} correspondingly. Analysis of variance (ANOVA) reveals that the $CH_3NH_3PbI_{3-x}Cl_x$ thickness is the most dominant input parameter affecting the PCE of the device. The optimized input parameters yield the maximum attainable PCE of 35.91% with a signal-to-noise ratio (SNR) of 31.11 dB.

Keywords: *Analysis of variance, Graphene oxide, Hole transport layer, Power conversion efficiency, Signal-to-noise ratio*

1. INTRODUCTION

Traditional energy sources are significant contributors to climate change and global warming, posing direct hazards to the current century due to their greenhouse emissions. Over the last half-century, there has been a global push towards swapping fossil fuels with renewable, ecologically safe, and sustainable alternatives. Solar energy is one of the most renowned renewable energy sources. Despite the fact that the early generation of silicon-based solar cells had a high power conversion efficiency (PCE) of 25%, they are costly to manufacture due to the large amount of energy required to refine the silicon. To address the cost issue, a new generation of solar cells based on lead (Pb) perovskite (PSCs) was invented. The theoretical efficiency of this type of cell has increased significantly over the previous decade, recently beyond 30% [1]–[4]. Graphene compounds have demonstrated potential in enhancing substrate protection, charge extraction, and defect passivation. Currently, thin layers of graphene oxide (GO) have been utilized as a hole transport layer (HTL) in perovskite solar cells, and the performances are considerably greater than technology produced utilizing PEDOT:PSS [5], [6]. The incorporation of graphene oxide (GO) in the perovskite layer of a PSC reduces series resistance (R_s). This was linked to improved crystallinity of the perovskite in the composite.

Additionally, surface potentials of a PSC were decreased with a rise of both J_{sc} and V_{oc} by reducing the highest occupied molecular orbital (HOMO) energy levels with the introduction of GO. GO offers considerable promise in overcoming some of the most severe shortcomings of optimizing PSCs. Despite this huge potential, the usage of graphene-based materials in PSCs is still in the underlying stages and, consequently, requires constant evaluation and study to unveil its potential comprehensively. For many decades, the SCAPS-1D software has been frequently employed in photovoltaic research to investigate the influence of material characteristics and device configurations on thin-film solar cell performance [7]–[9]. Ali and Karim (2022) reported a computer -simulation study on a thin-film solar cell based on a p-type CCZTSe-absorbent -layer using SCAPS-1D [10]. They found that increasing 26.94% of the thickness of the (CCZTSe) layer results in an increase in PCE, from 23.27 to 26.66%. Azza *et al.* (2023) employed SCAPS-1D to study the behavior of solar cells based on GaAs p-i-n GaAs configuration [11]. Their findings demonstrated that the behavior of the investigated devices is directly proportional to temperature and layer thickness. Lam (2020) utilized SCAPS-1D to perform numerical modeling of ZnO/CuO/Cu_2O thin-film solar cells [12]. The thickness and donor density of CuO and ZnO layers were thoroughly examined and analyzed.

The results indicated that the best structure of a ZnO/CuO/Cu_2O thin-film solar cell can be achieved when the ZnO layer thickness, CuO layer thickness, and donor density in the ZnO layer are, respectively, 100 nm, 500 nm, and $1x10^{17}$ cm^{-3}. Muhammed *et al.* (2021) studied the impact of design parameters on tin-based perovskite solar cells via SCAPS-1D [13]. The study was conducted by adjusting the doping concentration of the perovskite absorption layer, its thickness, the electron affinities of the electron transport layer (ETL) and the hole transport layer (HTL), as well as the defect density of the perovskite absorption layer and the hole mobility of the HTL. The final results demonstrate that the ecologically friendly, lead-free perovskite solar cell is a viable solar cell configuration with a high theoretical efficiency of 20.35%. On the basis of these previous studies, it can be concluded that SCAPS-1D is a valuable numerical simulation tool for the theoretical analysis of numerous thin-film solar cell configurations that can provide insight into the internal physics of solar cells as well as parameter guidance for the fabrication of actual devices.

The objective of optimization is to produce the "ideal" design compared to a set of prioritized criteria or constraints. These include optimizing aspects such as productivity, strength, dependability, lifespan, efficiency, and usage. In terms of the solar cell design point of view, optimization may be deployed to identify the ideal configuration of design parameters to attain optimum device performance. Rahal *et al.* (2022) conducted a study to optimize materials for the Back Surface Field (BSF) layer in Heterojunction with Intrinsic thin layer (HIT) solar cells [14]. The results indicated a substantial efficiency of 27.44%, stressing the necessity of utilizing hydrogenated amorphous silicon instead of crystalline silicon to build the BSF layer, as is the case for typical HIT solar cells. Manzoor *et al.* (2022) presented a work to optimize the indium gallium nitride p-n junction solar cells for the highest possible PCE [15]. The thickness and carrier density of p- and n-In_x $Ga_{1-x}N$ layers were optimized via numerical simulation. The results demonstrated that the PCE is more susceptible to the fluctuations of layer thickness and carrier density of the top p-In_x $Ga_{1-x}N$ layer than the bottom n-In_x $Ga_{1-x}N$ layer. Apart from that, the results also revealed that the thinner p-In_x $Ga_{1-x}N$ layer with higher carrier density delivers superior PCE.

Design of Experiments (DoE) offers quantitative statistical optimization methodologies and their implementation to engineering design, development, production, and operational processes. Mohammed and Fahim (2020) deployed the Response Surface Methodology (RSM) of DoE to optimize the PCE of a tandem organic solar cell [16]. The optimization procedure is carried out by developing an analytical polynomial regression model correlating the PCE to the thicknesses of the active layers. The outcomes demonstrated that the optimized thickness successfully increased the PCE by 47.7%. Makableh *et al.* (2021) similarly employed RSM-DoE to study the influence of coating silicon solar cells with zinc oxide, aluminum oxide and titanium dioxide nanostructures on the optical performance of the cells [17]. The results suggested that ZnO nanoparticles were the best choice for an anti-reflective coating on Silicon, as they gave the lowest reflection values among the three nanostructured materials. Using ZnO nanoparticles with a radius of 38 nm, the optimal conditions for achieving minimal surface reflections for silicon solar cells were successfully discovered.

Oktiawati *et al.* (2017) proposed the application of the Taguchi DoE in the design optimization of Dye Solar Cells (DSC) for enhanced performance [18]. The findings suggested that the ideal design of DSC is 10µm of TiO_2, $90m^2/g$ of TiO^2 photoelectrode surface area, 1M of iodide concentration in the electrolyte, and two layers with 20nm of TiO_2 passivation layer thickness, with an efficiency of ~4.6%. Bahrudin *et al.* (2018) also applied L_9 Taguchi DoE to determine the optimal values for three material parameters: Copper Telluride (CuTe), Perovskite absorber layer ($CH_3NH_3PbI_3$) and Cadmium Sulfide (CdS) to achieve the highest V_{oc} and J_{sc} values [19]. Post-Taguchi optimization demonstrated that the Perovskite Solar Cell had successfully reached 20.7% average PCE. Bahrudin *et al.* (2020) employ Taguchi DoE to explore the impact of the absorber layer grading profile on the photovoltaic performance of CIGS solar cells [20]. The improved device achieved an average efficiency of 22.08% with equivalent J_{sc}, V_{oc} and FF measured at 43.05 mA/cm^2, 0.704V and 76.37%, correspondingly. Based on this past research, it is possible to infer that DoE approaches are useful in forecasting the optimal design parameters of solar cells for ideal theoretical performance.

As a response, the L_{32} (2^8) Taguchi design will be used in this work, in which eight input (material) parameters will be examined and optimized for improved PCE of Graphene-based Perovskite solar cells. Signal-to-noise ratio (SNR) analysis will be conducted to identify the ideal input parameter values that would yield the maximum PCE of the device. Meanwhile, the analysis of variance (ANOVA) will be conducted to reveal the importance of each input parameter upon PCE variations.

2. METHODOLOGY

Device simulation and modeling in this study are conducted using a one-dimensional solar cell capacitance simulator (SCAPS-1D) and L_{32} (2^8) Taguchi design. Basically, the SCAPS-1D simulator is used to conduct solar cell simulations to attain important output characteristics such as J_{sc}, V_{oc}, FF, and PCE. Additionally, the input parameters of graphene-based PSCs are appropriately modeled using the L_{32} ($2^{8)}$ Taguchi design in order to achieve greater PCE. This study employs 1D Solar Cell Capacitance Simulator (SCAPS-1D) to simulate the PSC with FTO/TiO_2/$CH_3NH_3PbI_{3-x}Cl_X$/GO/counter electrode configuration in which the FTO, TiO_2, $CH_3NH_3PbI_{3-x}Cl_X$, and GO represents fluorine-doped tin oxide, titanium dioxide, mixed halide perovskite and graphene oxide respectively. FTO serves as transparent conducting oxide (TCO), typically employed for blocking photovoltaic light.

Large bandgaps with higher energy than visible light are present in transparent materials. $CH_3NH_3PbI_{3-x}Cl_X$

perovskite serves as a light absorber that has outstanding light absorption, charge-carrier mobility, and lifetimes, leading to high power conversion efficiency (PCE). TiO_2 is adopted as the electron transport layer (ETL) predominantly due to its uniform layer with tiny microstructures that increase the surface area of the under-layer and raise the overall efficiency of the cells. ETL performs a major function in collecting and transporting photo-generated electron transport and acts as a hole-blocking layer by preventing recombination rate. On the other hand, GO functions as the hole transport layer (HTL), restricting the passage of electrons in the opposite manner of the electron transport layer (ETL). GO is regarded as an ideal HTL candidate that features organically high hole mobility, and energy levels that are compatible with the perovskite layer. There are several input parameters involved in this PSC simulation, which are listed in Table 1. Figure 1 and Figure 2 show the layer arrangement and its corresponding energy band diagram employed in this study.

Table 1 Input parameters used in the simulation work

Input Parameter	**TCO**	**ETL**	**Absorber**	**HTL**
	FTO	**TiO_2**	**$CH3NH_3PbI_{3-x}Cl_x$**	**GO**
Thickness (μm)	0.1	0.03	0.9	0.03
Bandgap (eV)	3.5	3.2	1.55	3.2
Electron affinity (eV)	4	4	3.9	1.9
Dielectric permittivity (relative)	9	100	6.5	3
Conduction band effective d-o-s (cm^{-3})	$2.2x10^{18}$	10^{19}	$2.2x10^{17}$	$2.2x10^{17}$
Valence band effective d-o-s (cm^{-3})	$1.8x10^{19}$	10^{19}	$1.8x10^{19}$	$1.8x10^{21}$
Electron thermal velocity (cm/s)	10^7	10^7	10^7	10^7
Hole thermal velocity (cm/s)	10^7	10^7	10^7	10^7
Electron mobility (cm^2/Vs)	20	6e-3	2	100
Hole mobility (cm^2/Vs)	10	6e-3	2	300
Shallow uniform donor density, N_D (cm^{-3})	$2x10^{19}$	10^{19}	10^{17}	-
Shallow uniform acceptor density, N_A (cm^{-3})	-	-	-	10^{20}
Defect density, Nt (cm^{-3})	10^{15}	10^{15}	10^{13}	10^{15}
Ref.	[1]	[1]	[1]	[6]

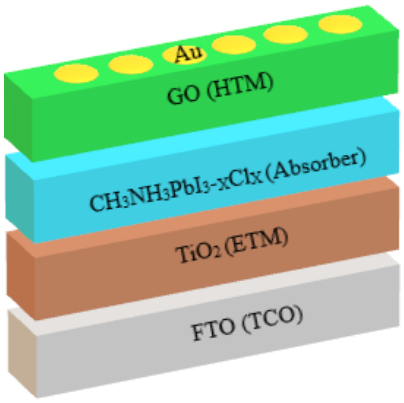

Figure 1. PSC's layer arrangement

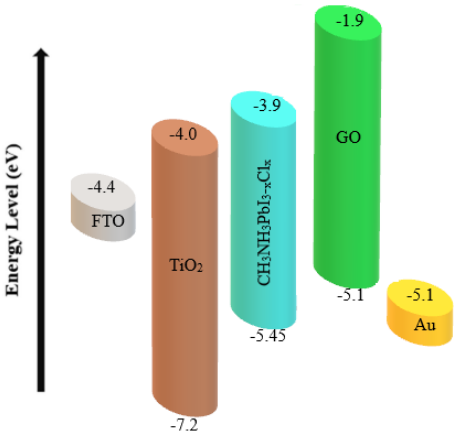

Figure 2. Energy band diagram of Graphene Oxide HTL Perovskite device

As an optical energy source for the simulation, the typical sun spectrum AM 1.5 is beamed to the front contact. The simulation resolves carrier transport, drift-diffusion, and recombination model to extract current density-voltage curves as the open circuit voltage (V_{oc}), short circuit current density (J_{sc}), fill factor (FF) and power conversion efficiency (PCE) can be retrieved and calculated. The output responses of the device, *FF*, and *PCE* are measured by using (1) and (2)[21], [22].

$$FF = \frac{V_{mp}J_{mp}}{V_{OC}J_{SC}} \quad (1)$$

$$PCE = \frac{J_{SC}\times FF\times V_{OC}}{P_{in}} \quad (2)$$

where V_{mp} and J_{mp} are voltage and current density at maximum power point, respectively. The fundamental objective of this simulation research employing low-cost materials renowned for their simple and fast processing is to attain the maximum achievable PCE.

In addition to the simulation approach, the input materials of the perovskite device will be modeled using the L_{32} (2^8) Taguchi design to get the best possible PCE. The perovskite device will be modeled based on the magnitude of eight input parameters: FTO thickness, FTO donor concentration, TiO_2 thickness, TiO_2 donor concentration, $CH_3NH_3PbI_{3-x}Cl_x$ thickness, $CH_3NH_3PbI_{3-x}Cl_x$ donor concentration, GO thickness and GO acceptor concentration in which each of them is denoted by A, B, C, D, E, F, G and H correspondingly. Table 2 shows two levels of magnitude are allocated to each of the input parameters.

Table 2 Input parameters and their levels

Symbol	Input Parameter	Unit	Level 1	Level 2
A	FTO thickness	µm	0.1	0.9
B	FTO donor concentration	cm^{-3}	$1x10^{11}$	$1x10^{20}$
C	TiO_2 thickness	µm	0.03	0.09
D	TiO_2 donor concentration	cm^{-3}	$1x10^{11}$	$1x10^{20}$
E	$CH_3NH_3PbI_{3-x}Cl_x$ thickness	µm	0.1	0.9
F	$CH_3NH_3PbI_{3-x}Cl_x$ donor concentration	cm^{-3}	$1x10^{11}$	$1x10^{20}$
G	GO thickness	µm	0.03	0.09
H	GO acceptor concentration	cm^{-3}	$1x10^{11}$	$1x10^{20}$

The principal objective of an orthogonal array (OA) is to decrease the number of tests required to determine the design's most influential components. The experimental data will be analyzed using the signal-to-noise ratio (SNR) and analysis of variance (ANOVA) [23]. In this work, the PCE of the PSC device is classified based on its higher-quality features. The higher-the-better quality characteristic is continuous and has a nonnegative quality attribute. The main objective is to maximize output response. The SNR is established so that the PCE is maximized to its greatest extent. The SNR for higher-the-better can be represented as [24]:

$$SNR_{higher-the-better} = -10log_{10}\left[\frac{1}{n}\sum_{i=1}^{n}\frac{1}{y_i^2}\right] \quad (3)$$

Where n is the number of experiments, and y_i is the experimental magnitude of PCE. The L_{32} (2^8) Taguchi design consists of 32 rows of experimental sets. Table 3 displays the experimental array of the L_{32} (2^8) Taguchi design for all input parameters.

3. RESULTS AND DISCUSSION

In this work, L_{32} (2^8) Taguchi design with numerical simulation is employed to simulate a Perovskite Solar Cell (PSC) using Graphene Oxide (GO) HTL. The L_{32} (2^8) Taguchi design is chosen primarily owing to the fact that the study comprises eight input parameters. The L_{32} (2^8) Taguchi design offers a condensed design of experiment (DoE) with 32 sets of experiments.

3.1. Analysis of signal-to-noise Ratio (SNR)

The purpose of the SNR response analysis is to calculate the signal-to-noise ratio (SNR) for all input process parameters. SNR is utilized to determine the optimum input parameters and to assess experimental results. For the PCE, the higher-the-better category is considered owing to its potential to optimize the value of the dependent variables as much as feasible. The 32 experiment sets have been run via L_{32} (2^8) Taguchi design, in which their corresponding PCE (output response) and computed SNR are recorded in Table 4.

Table 3 L_{32} (2^8) Taguchi Design

Exp. No.	Level of Input Parameters							
	A	B	C	D	E	F	G	H
1	1	1	1	1	1	1	1	1
2	1	1	1	1	2	1	2	2
3	1	1	1	2	1	2	1	2
4	1	1	1	2	2	2	2	1
5	1	1	2	1	1	2	2	1
6	1	1	2	1	2	2	1	2
7	1	1	2	2	1	1	2	2
8	1	1	2	2	2	1	1	1
9	1	2	1	1	1	2	2	2
10	1	2	1	1	2	2	1	1
11	1	2	1	2	1	1	2	1
12	1	2	1	2	2	1	1	2
13	1	2	2	1	1	1	1	2
14	1	2	2	1	2	1	2	1
15	1	2	2	2	1	2	1	1
16	1	2	2	2	2	2	2	2
17	2	1	1	1	1	2	2	2
18	2	1	1	1	2	2	1	1
19	2	1	1	2	1	1	2	1
20	2	1	1	2	2	1	1	2
21	2	1	2	1	1	1	1	2
22	2	1	2	1	2	1	2	1
23	2	1	2	2	1	2	1	1
24	2	1	2	2	2	2	2	2
25	2	2	1	1	1	1	1	1
26	2	2	1	1	2	1	2	2
27	2	2	1	2	1	2	1	2
28	2	2	1	2	2	2	2	1
29	2	2	2	1	1	2	2	1
30	2	2	2	1	2	2	1	2
31	2	2	2	2	1	1	2	2
32	2	2	2	2	2	1	1	1

Based on Table 4, experiment row no.10 demonstrates the maximum SNR, recorded at 31.0631 dB. Linear model analysis for SNR is conducted to explain the relationship between one dependent variable (PCE) and eight independent variables (input parameters). Table 5 shows the estimated model coefficients for SNR.

S is the standard deviation of the contrast between the data points and the fitted points. S is quantified in the response's elements. S is used to evaluate the model's ability to describe the SNR of the PCE values. S is calculated in terms of the SNR of PCE values and indicates the divergence of the observed data points from the calculated data points. The smaller the S is, the more accurately the model explains the PCE variations.

Nevertheless, a lowered S value does not always imply the model's assumptions are met. To verify the assumptions, a plot of residual is required. Figure 3 depicts the model's normal probability plot. In this case, the input variables that contribute to the percentage increase of PCE values are required to be analyzed. S is computed as 0.2445 when the model is limited to its important predictors. This result suggests that the S value of data points surrounding the fitted values is 0.2445. If the models are compared, numbers less than 0.2445 imply a better fit, whereas values more than 0.2445 indicate an inadequate fit.

Table 4 PCE And SNR of L_{32} (2^8) Taguchi Design

Exp. No.	Level of Input Parameters								PCE	SNR
	A	B	C	D	E	F	G	H		
1	1	1	1	1	1	1	1	1	15.66	23.8958
2	1	1	1	1	2	1	2	2	27.85	28.8965
3	1	1	1	2	1	2	1	2	18.3	25.249
4	1	1	1	2	2	2	2	1	34.87	30.849
5	1	1	2	1	1	2	2	1	17.91	25.0619
6	1	1	2	1	2	2	1	2	34.51	30.7589
7	1	1	2	2	1	1	2	2	15.56	23.8402
8	1	1	2	2	2	1	1	1	27.45	28.7708
9	1	2	1	1	1	2	2	2	18.59	25.3856
10	1	2	1	1	2	2	1	1	35.74	31.0631
11	1	2	1	2	1	1	2	1	15.97	24.0661
12	1	2	1	2	2	1	1	2	28.94	29.23
13	1	2	2	1	1	1	1	2	15.91	24.0334
14	1	2	2	1	2	1	2	1	28.2	29.005
15	1	2	2	2	1	2	1	1	18.4	25.2964
16	1	2	2	2	2	2	2	2	35.63	31.0363
17	2	1	1	1	1	2	2	2	17.22	24.7207
18	2	1	1	1	2	2	1	1	32.76	30.3069
19	2	1	1	2	1	1	2	1	14.65	23.3168
20	2	1	1	2	2	1	1	2	26.13	28.3428
21	2	1	2	1	1	1	1	2	14.6	23.2871
22	2	1	2	1	2	1	2	1	25.23	28.0383
23	2	1	2	2	1	2	1	1	17.15	24.6853
24	2	1	2	2	2	2	2	2	32.82	30.3228
25	2	2	1	1	1	1	1	1	15.79	23.9676
26	2	2	1	1	2	1	2	2	28.65	29.1425
27	2	2	1	2	1	2	1	2	18.4	25.2964
28	2	2	1	2	2	2	2	1	35.43	30.9874
29	2	2	2	1	1	2	2	1	18.07	25.1392
30	2	2	2	1	2	2	1	2	35.27	30.9481
31	2	2	2	2	1	1	2	2	15.65	23.8903
32	2	2	2	2	2	1	1	1	28	28.9432

Table 5 Estimated model coefficients for SNR

Term	Coef	SE Coef	T	P
Constant	27.1179	0.04322	627.458	0.000
A	0.1595	0.04322	3.690	0.001
B	-0.2215	0.04322	-5.125	0.000
C	0.0518	0.04322	1.200	0.243
D	-0.0148	0.04322	-0.341	0.736
E	-2.6722	0.04322	-61.829	0.000
F	-0.8263	0.04322	-19.118	0.000
G	0.0118	0.04322	0.272	0.788
H	-0.0309	0.04322	-0.714	0.482
Model Summary				
S	R-Sq		R-Sq(adj)	
0.2445	99.46%		99.27%	

R-squared (R-Sq) is the proportion of PCE variance explicated by the model. The error sum of squares represents the variance that cannot be explained by the model (which is the total variation in the model). R-squared is utilized to evaluate how well the model matches the data points. The greater the R-Sq number, the more closely the model matches the data.

R-Sq always ranges between 0% and 100%. In this case, both R-Sq and R-Sq(adj) are fairly high at 99.46% and 99.27%, respectively, indicating that all the input parameters provide a great model. According to Table 6, the SNR of 32 orthogonal experiment sets is separated into level 1 and level 2 of input parameters. A greater SNR will lead to a greater PCE. The greater the SNR, the greater the PCE. The emphasis must be centered on minimizing noise sensitivity by maximizing SNR.

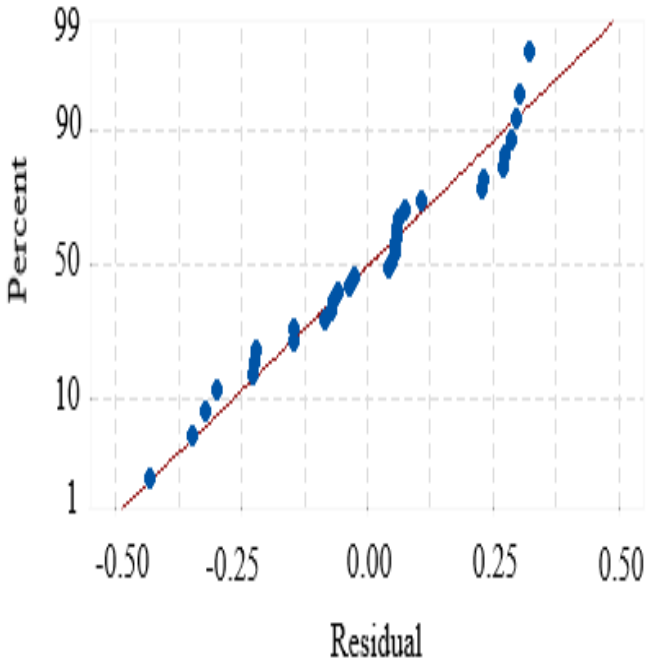

Figure 3. Normal probability plot for SNR

Table 6 Higher-the-better SNR response for PCE

Sym.	Input Parameter	SNR (Higher-the-better)		Delta	Rank
		Level 1	Level 2		
A	FTO thickness	27.28	26.96	0.32	4
B	FTO donor concentration	26.90	27.34	0.44	3
C	TiO_2 thickness	27.17	27.07	0.10	5
D	TiO_2 donor concentration	27.10	27.13	0.03	7
E	$CH_3NH_3PbI_{3-x}Cl_x$ thickness	24.45	29.79	5.34	1
F	$CH_3NH_3PbI_{3-x}Cl_x$ donor concentration	26.29	27.94	1.65	2
G	GO thickness	27.13	27.11	0.02	8
H	GO acceptor concentration	27.09	27.15	0.06	6

The input parameter effects plot for SNR (Higher-is-Better) is constructed based on the information in Table 6, as shown in Figure 4. The dashed reference lines in the graph indicate the overall mean SNR (higher is better) of 27.118 dB. Based on their maximum SNR, input parameters A1, B2, C1, D2, E2, F2, G1, and H2 have been selected as the optimal values for the highest PCE.

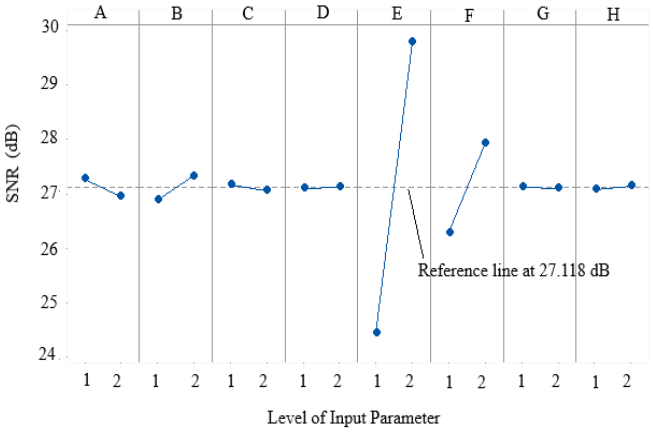

Figure 4. Input parameter effects plot for SNR (Higher-is-Better)

3.2. Analysis of variance (ANOVA)

Analysis of variance (ANOVA) is a basic statistical technique used to determine whether input process factors have a significant impact on the performance characteristic. ANOVA is technically defined as the breakdown of variance, which serves as a tool for gaining a better understanding of the relative influence of the various components. ANOVA is also necessary for quantifying the error of variance for input parameter effects and the error of variance for prediction. Table 7 presents the ANOVA findings for the L_{32} (2^8) Taguchi design. Figure 5 depicts the percentage contributions for each input parameter that influences the SNR.

Table 7 Result of ANOVA for the L_{32} (2^8) Taguchi design

Input Parameter	DF	Seq SS	Adj SS	Adj MS	F	P	Input parameter effects on SNR (%)
A	1	0.814	0.814	0.814	13.61	0.0032018	0.32018
B	1	1.570	1.570	1.570	26.26	0.006175462	0.617546
C	1	0.086	0.086	0.086	1.44	0.000338274	0.033827
D	1	0.007	0.007	0.007	0.12	2.75339E-05	0.002753
E	1	228.5	228.5	228.5	3822.9	0.898781428	89.87814
F	1	21.847	21.847	21.847	365.51	0.085933321	8.593332
G	1	0.004	0.004	0.004	0.07	1.57337E-05	0.001573
H	1	0.030	0.030	0.030	0.51	0.000118002	0.0118
Residual Error	23	1.375	1.375	0.060		0.005408446	0.540845
Total	31	254.232				1	100

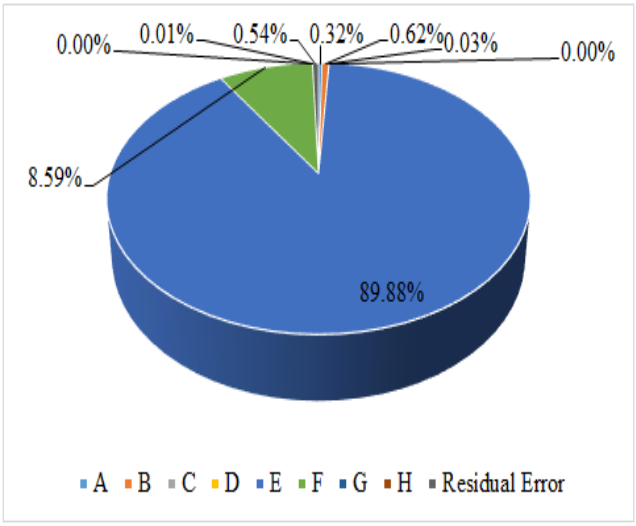

Figure 5. Percentage contributions of input parameter on the SNR for Graphene Oxide HTL PSC device

The pie chart reveals that the $CH_3NH_3PbI_{3-x}Cl_x$ thickness (input parameter E) variations have the greatest influence on the SNR of a Graphene Oxide HTL PSC device. The $CH_3NH_3PbI_{3-x}Cl_x$ thickness accounts for 89.88% of the input parameter influence on SNR, making it the most influential input parameter on the PCE of a Graphene Oxide HTL PSC device. The donor concentration of $CH_3NH_3PbI_{3-x}Cl_x$ (input parameter F) is considered the second-most significant input parameter, contributing 8.59% to SNR.

The other input parameters can be considered insignificant because their value changes have hardly any effect on PCE.

3.3. Verification test

The purpose of the verification test is to check that the optimal level of input parameters predicted by the L_{32} (2^8) Taguchi design produces the expected simulation outcome. The Graphene oxide HTL PSC device is simulated using the predicted level of input parameters previously revealed in Figure 4. Figure 6 depicts a comparison of the device's J-V transfer characteristics before and after optimal modeling.

After optimal modeling, the V_{oc} of the device has improved by 10.22%, with measured values of 1.4263 V (before optimal modeling) and 1.5285 V (after optimal modeling). Besides, the J_{sc} has boosted from 13.06 mA/cm^2 to 25.68 mA/cm^2 as a result of optimal modeling with a 49.1% improvement. It is mostly attributable to greater resistive losses caused by the dominant influence of $CH_3NH_3PbI_{3-x}Cl_x$ thickness variations. The input parameter levels and the simulation outputs of the Graphene Oxide HTL PSC device before and after the optimal modeling are summarized in Table 8.

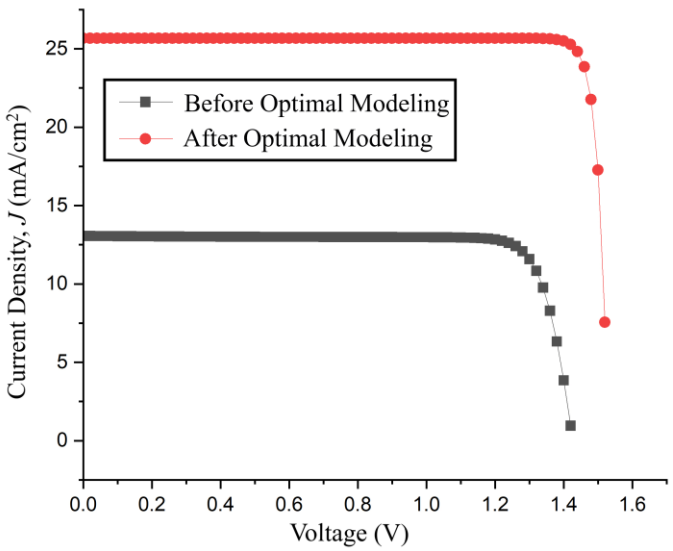

Figure 6. Overlay of J-V transfer characteristic of graphene oxide HTL PSC device before and after optimal modeling

Table 8 Summary of Optimal Modeling of Graphene Oxide HTL PSC Device

Symbol	Input parameter	Units	Before optimal modeling (First experiment row)	After optimal modeling
A	FTO thickness	µm	0.1	0.1
B	FTO donor concentration	cm^{-3}	$1x10^{11}$	$1x10^{20}$
C	TiO_2 thickness	µm	0.03	0.03
D	TiO_2 donor concentration	cm^{-3}	$1x10^{11}$	$1x10^{20}$
E	$CH_3NH_3PbI_{3-x}Cl_x$ thickness	µm	0.1	0.9
F	$CH_3NH_3PbI_{3-x}Cl_x$ donor concentration	cm^{-3}	$1x10^{11}$	$1x10^{20}$
G	GO thickness	µm	0.03	0.03
H	GO acceptor concentration	cm^{-3}	$1x10^{11}$	$1x10^{20}$
Power conversion efficiency (PCE)		%	15.66	35.91
Signal-to-noise ratio (SNR) for higher-the-better		dB	23.9	31.11

4. CONCLUSION

Perovskite Solar Cell with Graphene Oxide HTL is successfully modeled using SCAPS 1D software and L_{32} (2^8) Taguchi design to boost the Graphene Oxide HTL PSC's performance. The primary purpose of this research is to model the device's input parameters to get a greater PCE. ANOVA demonstrates that the $CH_3NH_3PbI_{3-x}Cl_x$ thickness variations are the most influential input parameter influencing the PCE, accounting for 89.88% of the input parameter influence on SNR. With 31.11 dB of SNR, the optimal input parameter has yielded the highest achievable PCE, measured at 35.91%, as predicted by the SNR analysis. The PCE has increased by 57.7%, suggesting that the L_{32} (2^8) Taguchi design is an effective approach for boosting the Graphene Oxide HTL PSC's performance.

ACKNOWLEDGMENTS

The authors would like to thank the Ministry of Higher Education (MOHE) for sponsoring this work under the project (FRGS/1/2022/TK07/UTEM/02/47) and MiNE, CeTRI, Faculty of Electronics and Computer Technology and Engineering (FTKEK), Universiti Teknikal Malaysia Melaka (UTeM) for the moral support throughout the project. The authors would also like to thank Dr. Marc Burgelman of the University of Gent in Belgium for supplying the SCAPS-1D simulation program.

REFERENCES

[1] M. Alla, V. Manjunath, N. Chawki, D. Singh, S. C. Yadav, M. Rouchdi, and F. Boubker, "Optimized CH3NH3PbI3-XClX based perovskite solar cell with theoretical efficiency exceeding 30%," *Optical Materials*, vol. 124, p. 112044, 2022.

[2] C. Ma and N. G. Park, "A Realistic Methodology for 30% Efficient Perovskite Solar Cells," *Chem*, vol. 6, no. 6, pp. 1254–1264, 2020.

[3] S. Kim, T. T. Trinh, J. Park, D. P. Pham, S. Lee, H. B. Do, N. N. Dang, V. A. Dao, J. Kim, and J. Yi, "Over 30% efficiency bifacial 4-terminal perovskite-heterojunction silicon tandem solar cells with spectral albedo," *Scientific Reports*, vol. 11, no. 1, p. 1–10, 2021.

[4] J. Diekmann, P. Caprioglio, et al., "Pathways towards 30% efficient perovskite solar cells," *Solar RRL*, vol. 5, no. 8, p. 1–13, 2021.

[5] G. A. Nowsherwan, A. Samad, M. A. Iqbal, T. Mushtaq, A. Hussain, M. Malik, S. Haider, P. V. Pham, and J. R. Choi, "Performance Analysis and Optimization of a PBDB-T:ITIC Based Organic Solar Cell Using Graphene Oxide as the Hole Transport Layer," *Nanomaterials*, vol. 12, no. 1767, p. 1–14, 2022.

[6] N. Touafek, R. Mahamdi, and C. Dridi, "Boosting the performance of planar inverted perovskite solar cells employing graphene oxide as HTL," *Digest Journal of Nanomaterials and Biostructures*, vol. 16, no. 2, pp. 705–712, 2021.

[7] A. Niemegeers and M. Burgelman, "Modelling of AC-Characteristics of Solar Cells," in *Proc. 25nd IEEE Photovoltaic Specialists Conference*, pp. 901–904, 1996.

[8] K. Decock, P. Zabierowski, and M. Burgelman, "Modeling metastabilities in chalcopyrite-based thin film solar cells," *Journal of Applied Physics*, vol. 111, p. 043703, 2012.

[9] M. Burgelman, K. Decock, S. Kheli, and A. Abass, "Advanced electrical simulation of thin film solar cells," *Thin Solid Films*, vol. 535, pp. 296–301, 2013.

[10] Ali, W. Y., Kareem, M. Q. (2022) "Simulation of Thin-Film Solar Cells based on (CCZTSe) Using (SCAPS-1D) Simulation of Thin-Film Solar Cells based on (CCZTSe) Using (SCAPS-1D) Program. *Journal of Algebraic Statistics*, vol. 13, no. 2, pp. 902–913.

[11] Azza, M., Chahid, E. H., Hmairrou, A., Abdia, R., Tridane, M., Malaoui, A., Belaaouad, S. (2023). Numerical Simulation of p-i-n GaAs Photovoltaic Cell Using SCAPS-1D. *Biointerface Research in Applied Chemistry*, vol. 13, no. 3, pp. 1–11, 2023.

[12] Lam, N. D. (2020). Modelling and numerical analysis of ZnO/CuO/Cu2O heterojunction solar cell using SCAPS. *Engineering Research Express*, vol. 2, no. 2, pp. 0–9, 2020.

[13] Muhammed, O. A., Eli, D., Boduku, P. H., Tasiu, J., Ahmad, M. S., Usman, N. (2021). Modeling and simulation of lead-free perovskite solar cell using scaps-1D," *East European Journal of Physics*, vol. 2021, no. 2, pp. 146–154.

[14] Rahal, W. L. Rached, D., Mahi, F., Azzemou, F. (2022). Simulation and Optimization of Back Surface Field for Efficient HIT Solar Cells. *Silicon*. vol. 14, no. 6, pp. 2999–3003.

[15] Manzoor, H. U., Kwan, T. A., Shiong, N. S., Hassan, Z. (2022). Carrier Density and Thickness Optimization of InxGa1-xN Layer by Scaps-1D Simulation for High Efficiency III-V Solar Cell. *Sains Malaysiana*, vol. 51, no. 5, pp. 1567–1576.

[16] A. R. Mohammed and I. S. Fahim, "Tandem Organic Solar Cell Optimization Using Response Surface Methodology," in *International Conference on Data Analytics for Business and Industry: Way Towards a Sustainable Economy*, (2020), pp. 1–5.

[17] Makableh, Y. F., Alzubi, H., Tashtoush, G. (2021). Design and optimization of the anti-reflective coating properties of silicon solar cells by using response surface methodology. *Coatings*, vol. 11, no. 6, pp. 1–13.

[18] Oktiawati, U. Y., Mohamed, N. M., Burhanudin, Z. A. (2017). Applications of Taguchi method for optimization of dye solar cell design," *Sains Malaysiana*, vol. 46, no. 3, pp. 503–508.

[19] M. S. Bahrudin, S. F. Abdullah, I. Ahmad, A. W. M. Zuhdi, A. H. Hasani, F. Za'abar, M. Malik, and M. N. Harif, "Jsc and Voc Optimization of Perovskite Solar Cell with Interface Defect Layer Using Taguchi Method," in *2018 IEEE International Conference on Semiconductor Electronics (ICSE)*, (2018), pp. 192–196.

[20] Bahrudin, M. S., Yusoff, Y., Abdullah, S. F., Zuhdi, A. W. M., Amin, N., Ahmad, I. (2020). A Parametric Optimization using Taguchi Method for Cu (In,Ga)(S,Se)2 Thin Film Solar Cell Device Simulation. *Journal of Energy and Environment*, vol. 12, no. 2, pp. 1–7.

[21] Green, M. A. (1981). Solar Cell Fill Factors: General Graph and Empirical Expressions. *Solid-State Electronics*, vol. 24, pp. 788–789.

[22] Jain, A., Kapoor, A. (2004). Exact analytical solutions of the parameters of real solar cells using Lambert W-function. *Solar Energy Materials and Solar Cells*. vol. 81, no. 2, pp. 269–277.

[23] Kaharudin, K. E., Salehuddin, F., Zain, A. S. M., Aziz, M. N. I. A., Ahmad, I. (2016). Application of Taguchi Method for Lower Subthreshold Swing in Ultrathin Pillar SOI VDG- MOSFET Device. *Journal of Advanced Research in Applied Sciences and Engineering Technology*, vol. 2, no. 1, pp. 30–43.

[24] M. S. Phadke, "Quality Engineering Using Robust Design", Pearson Education, (2001) pp. 73-74.